# DECREASING SUNSPOT MAGNETIC FIELDS EXPLAIN UNIQUE 10.7 cm RADIO FLUX

W. LIVINGSTON[1], M. J. PENN[1], AND L. SVALGAARD[2]
[1] National Solar Observatory, 950 North Cherry Avenue, Tucson, AZ 85718, USA
[2] HEPL, Via Ortega, Stanford University, Stanford, CA 94305, USA

## ABSTRACT

Infrared spectral observations of sunspots from 1998 to 2011 have shown that on average sunspots changed, the magnetic fields weakened, and the temperatures rose. The data also show that sunspots or dark pores can only form at the solar surface if the magnetic field strength exceeds about 1500 G. Sunspots appear at the solar surface with a variety of field strengths, and during the period from 1998 to 2002 a histogram of the sunspot magnetic fields shows a normal distribution with a mean of $2436 \pm 26$ G and a width of $323 \pm 20$ G. During this observing period the mean of the magnetic field distribution decreased by $46 \pm 6$ G per year, and we assume that as the 1500 G threshold was approached, magnetic fields appeared at the solar surface which could not form dark sunspots or pores. With this assumption we propose a quantity called the sunspot formation fraction and give an analytical form derived from the magnetic field distribution. We show that this fraction can quantitatively explain the changing relationship between sunspot number and solar radio flux measured at 10.7 cm wavelengths.

*Key words:* Sun: infrared – sunspots

*Online-only material:* color figure

## 1. INTRODUCTION

During a roughly 11 year period, the number of sunspots seen on the solar disk shows a cyclic change. The current sunspot cycle (Cycle 24) has been strangely slow to develop, but even more strange is that infrared measurements of the central dark sunspot umbral regions have shown a decrease in the maximum magnetic field strength (with an associated temperature increase) since 1998 (Livingston 2002; Penn & Livingston 2006, 2011). This is different from visible light studies of solar-cycle-related sunspot magnetic field changes (Maltby et al. 1986; Mathew et al. 2007; Wesolowski et al. 2008; Penn & MacDonald 2007; Pevtsov et al. 2011; Watson & Fletcher 2011). Work by Rezaei et al. (2012) combines a small number of Fe I 1565 nm observations (99) with 132 measurements from different infrared spectral lines. These other two spectral lines have magnetic resolutions (given by $g$ times $\lambda$) equal to the visible Fe I 630 nm line, a factor of 2.9 lower than the resolution of the Fe I 1565 nm line. Like visible light studies, their work finds a solar-cycle magnetic change. In recent years, radio observations of solar emission at 10.7 cm wavelengths show a systematic increase compared to the sunspot number, something not seen in the previous years of these observations. In this Letter, we quantitatively examine the magnetic field and radio observations using a new idea about the emerging magnetic flux in the solar cycle, and we note how extrapolating this recent behavior points to a very small sunspot number for Cycle 25.

Determining the Zeeman wavelength splitting of the absorption line components using spectra provides the most reliable magnetic measurement in sunspots, and of the well-studied solar spectral lines the iron absorption line at 1565 nm is the best line to use for this measurement. A sample spectrum is shown in Figure 1. It is thought that this line is formed very near the solar surface, at a level in the photosphere of $z = 100$ km (Stenflo et al. 1987; Bruls et al. 1991), and the spectral line is rather insensitive to solar temperature changes. Thus, our set of 2700 ground-based measurements of sunspot umbral magnetic field strengths using this spectral line from the National Solar Observatory's[3] McMath-Pierce telescope on Kitt Peak has more magnetic sensitivity than other ground- and space-based sunspot magnetic field measurements.

## 2. DISTRIBUTION OF UMBRAL MAGNETIC FIELD STRENGTHS

During about 300 observing days over the past 13 years, infrared intensity spectra were collected from the darkest regions of the umbrae in the sunspots visible on the solar disk. The wavelength splitting of the $\sigma$-components gives the total magnetic field strength independent of view angle, and with this spectral line the splitting is fully resolved for field strengths greater than about 1100 G. The darkest areas correspond to the maximum magnetic field in the sunspot, and these observations have shown that the maximum magnetic field in sunspots has been decreasing in strength. Associated with this magnetic decrease is a corresponding increase in sunspot brightness as shown in Figure 2. As sunspots approach a brightness equal to the surrounding quiet Sun, they fade from view. Previous work with these data (Penn & Livingston 2006, 2011) has shown that sunspots are also increasing in temperature, as revealed by a drop in the abundance of OH molecules inside the sunspots, and the magnetic fields, intensities, and molecular abundances are changing in a manner consistent with previous studies of these quantities. The physics of sunspot formation is not being altered; for a given magnetic field strength, a sunspot forms at the surface with a temperature and brightness consistent with historical measurements (Schad & Penn 2010).

These data also show that for even the smallest dark feature observed (i.e., a pore or a sunspot without any penumbra) the magnetic field strength is always greater than about 1500 G. There are a few sunspot magnetic field measurements below 1500 G as shown in Figure 2 so this is not an exact value for the threshold, but we use it here as a convenient value. A

---

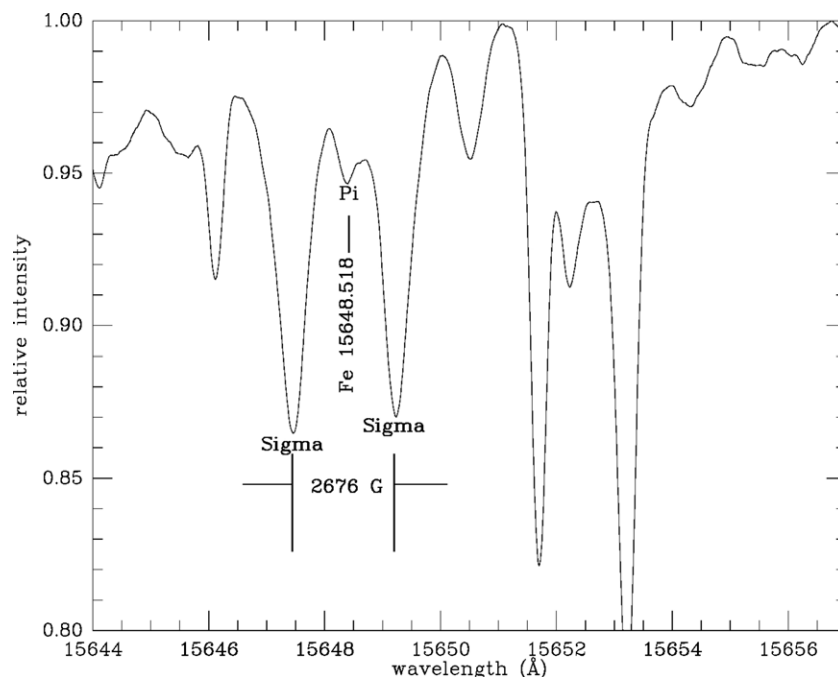[3] NSO is operated by AURA, Inc., under contract to the National Science Foundation.

**Figure 1.** Sample infrared intensity spectrum from a sunspot umbra showing the Zeeman splitting of the two components of the 15648 Å Fe I absorption line. The sunspot magnetic field required to produce this splitting is 2676 G.
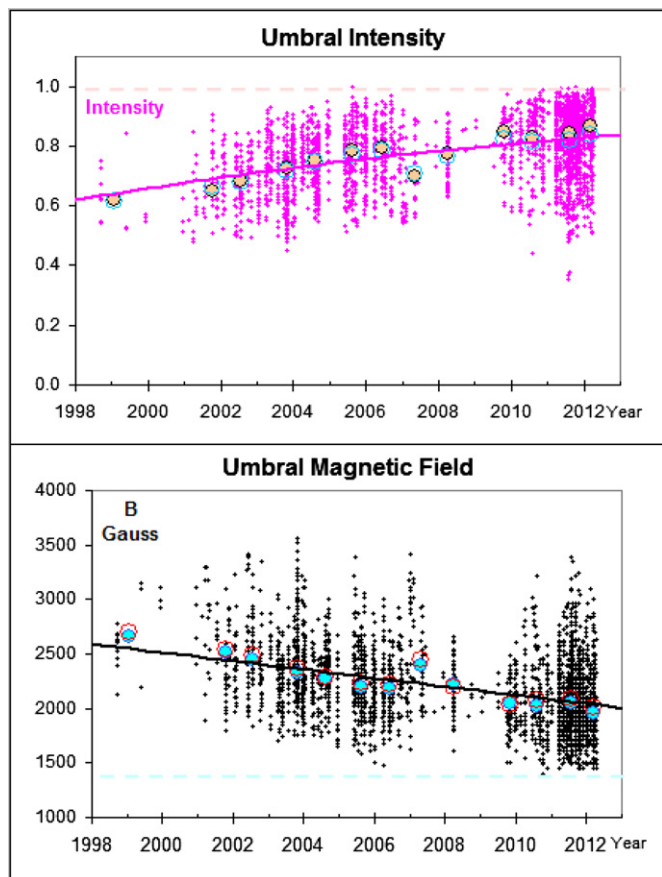


**Figure 2.** Changes in sunspot umbral intensity and maximum magnetic field. The intensity is normalized to the brightness of the nearby quiet Sun, and so a sunspot would disappear (it would have zero contrast) when $I$ reached a value of 1.0 on this graph. Similarly, dark sunspots do not appear with a maximum magnetic field strength below 1500 G.

(A color version of this figure is available in the online journal.)

detailed fit to the relation between the magnetic field strength and the sunspot intensity (relative to the quiet Sun) shows that for magnetic fields below about 1500 G ($1463 \pm 13.3$ G) a sunspot would have the same intensity as the surrounding Sun (Schad & Penn 2010). Because a magnetic field strength of 1500 G would imply an equipartition gas pressure of about 9000 N m$^{-2}$ ($9 \times 10^4$ dyne cm$^{-2}$) which corresponds to the modeled gas pressure at a height of about 40 km (roughly the height of formation of the 1565 nm Fe I absorption line) (Fontenla et al. 2007), it is not surprising that only magnetic fields larger than this value would dominate gas dynamics on the solar surface and form a dark pore or sunspot. Finally, recent measurements of small bright magnetic plage on the solar surface show a maximum magnetic field of 1450 G (Lagg et al. 2010), and generally fields below 1200 G (Kobel et al. 2011) are consistent with the proposal that only fields above 1500 G form dark spots.

Figure 3 shows a sequence of histograms produced from the magnetic field measurements from 1998 to 2011. It is important to note that these measurements include sunspots from the rise phase, maximum, decay phase and minimum of Cycle 23, and from the rise phase of Cycle 24. The data are binned in five-year intervals, except for the most recent observations which are binned over four years, resulting in three histograms. The observations show two characteristics: first, the distribution of magnetic field strengths measured in sunspots appears to be nearly a normal distribution across the observing period, and second that the magnetic field strength is shifting to smaller values in more recent times. A normal distribution fit to the 1998–2002 distribution reveals a mean of $2436 \pm 26$ G and a width of $323 \pm 20$ G ($1\sigma$ error values). The 1998–2002 and the 2003–2007 distributions are well approximated by a normal distribution, but by comparing the aligned distributions the 2008–2011 data show a lack of sunspots with the weakest field strengths, corresponding to magnetic fields below the 1500 G threshold. Fitting each distribution with a normal distribution shows that the 2003–2007 distribution is fit with a mean of $2204 \pm 10$ G and a width of $296 \pm 7$ G, while the 2008–2011
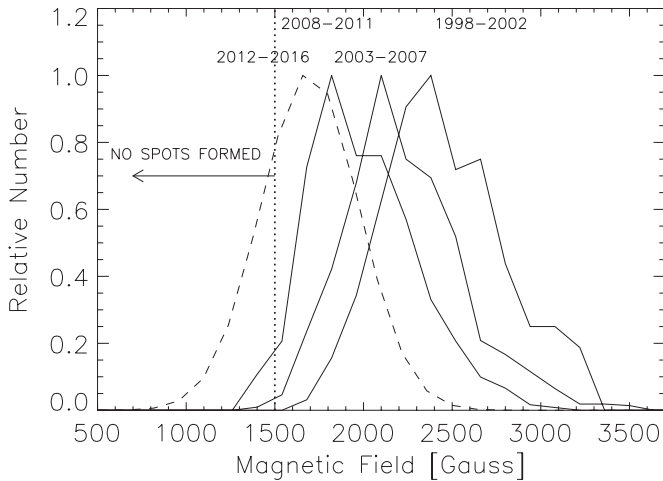
**Figure 3.** Observed magnetic field distributions from the IR spectral measurements from 1998 to 2011. The data are binned into three periods and labeled. The distributions are fit well with normal distributions and show a mean magnetic field decrease of $46 \pm 6$ G per year. The 1500 G magnetic field threshold (below which no dark spots are observed) is also plotted. The normal fit for the 1998–2002 data is shifted by the observed magnetic field change to predict the distribution for the period from 2012 to 2016, and about one-half of these magnetic fields will lie below the 1500 G spot formation threshold field strength.
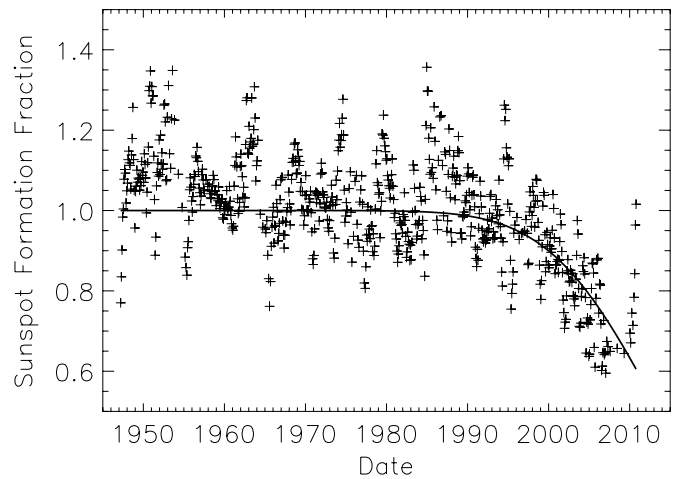


**Figure 4.** Sunspot formation fraction is defined as the number of sunspots seen on the solar surface divided by the number of sunspots predicted by the solar radio emission at 10.7 cm. The value is $1.0 \pm 0.11$ from 1947 through about 1995, and then it shows a statistically significant decline. It is least-squares fit with an $\mathrm{erf}(x)$ function, and it independently confirms the rate of change of the sunspot magnetic field strengths and the 1500 G threshold. Extrapolating this function into the future would predict about 50% fewer spots in Cycle 24 than seen in Cycle 23, and almost no spots in Cycle 25.

distribution best fit shows a mean of $1999 \pm 13$ G and a width of $276 \pm 9$ G. The distribution means have been moving to weaker field strengths at an average rate of $46 \pm 6$ G per year. This is a unique finding, as both the decreasing mean and the consistency over time contradict previous measurements of sunspot magnetic field change using shorter wavelength spectral lines, where sunspot magnetic fields and their proxies were thought to increase through the sunspot cycle, and abruptly decrease during sunspot minimum (Maltby et al. 1986; Mathew et al. 2007; Wesolowski et al. 2008; Penn & MacDonald 2007; Pevtsov et al. 2011; Watson & Fletcher 2011). Finally, Figure 3 shows a predicted distribution for future magnetic field measurements from 2012 to 2017, and it is clear that a significant fraction of the magnetic fields from this distribution would be below the 1500 G threshold for sunspot formation.

## 3. THE SUNSPOT FORMATION FRACTION

If the shape of this magnetic field distribution remains unchanged but the mean simply shifts to lower field strengths, measurements of sunspot magnetic fields will be unable to properly sample this distribution as the lower threshold value is encountered. Another method for measuring the emerging magnetic fields must be used, and one candidate is the radio emission from the Sun measured at a wavelength of 10.7 cm (F10.7). The values of F10.7 have been systematically recorded since 1947, and the flux shows a solar-cycle dependence, with more emission during solar maximum. This emission is thought to arise from a density-dependent emission which is enhanced in magnetic active regions, and from a gyrosynchrotron emission which is enhanced in regions of strong coronal magnetic fields. In addition to these active region components, there is a quiet component to F10.7 which produces a non-zero emission during the minimum phase of each sunspot cycle (Tapping & DeTracey 1990). The monthly averaged F10.7 can be fit with the monthly averaged sunspot number (SSN; the F10.7 flux values were taken from http://www.spaceweather.ca/sx-11-eng.php and the SSN data were used from http://sidc.oma.be/sunspot-data/dailyssn.php),

but the two are not linearly related. Since the value of SSN can drop to zero during solar minimum and F10.7 does not, this relationship becomes complicated for low SSN values. At large values of SSN and F10.7 the relationship becomes dominated by just a few data points. To simplify our fitting, we limit our fit to values of SSN in the range $10 < \text{SSN} < 210$, we include data from all years, and fit with only a second-order polynomial. The resulting coefficients ($59.8 \pm 1.3$, $0.95 \pm 0.03$, $(-2.1 \pm 1.7)\ 10^{-4}$) are in good agreement with fits from other authors (Johnson 2011; Thompson 2011). These limits are used throughout the following discussions, but it is important to note that by including a wider range of SSN values and using a higher-order polynomial fit we find the same results as this simpler analysis procedure.

Using the relationship between F10.7 and SSN, we can predict a monthly SSN value from each month's F10.7 emission, and we examine the ratio of this predicted SSN versus the observed SSN. Figure 4 plots the measured SSN divided by this F10.7 predicted value, and we call this value the sunspot formation fraction. From 1947 through 1995, this value was close to 1.0, with a standard deviation of about $\pm 0.14$. After that however, the ratio dips below 1.0, consistent with there being a lack of sunspots visible on the solar surface compared to the observed F10.7. The significance of this decrease can be tested with a nonparametric Spearman rank test, and we can test the significance of these derived Spearman coefficients by shuffling the data many times and computing the coefficients for these randomized data (Press et al. 1992; Bahcall et al. 1987). The decrease has a Spearman coefficient of $-0.55$, and the standard deviation of the Spearman coefficients for 1000 random shufflings of the data is only 0.09, indicating that the decrease involves a very significant deviation of $6\sigma$; and in comparison, the uptick at the end of 2011 shows a significance of only $2\sigma$.

We can quantitatively examine the time change of the sunspot formation fraction with two assumptions. Our first assumption is that the fraction of sunspot forming magnetic flux can be computed by integrating the sunspot magnetic field distribution above the 1500 G threshold and normalizing it by the integral

of the entire magnetic distribution. This numerator has the analytical form of the complementary error function, erfc($x$), which equals the integral of a normal distribution with a Gaussian width of unity from the argument $x$ to positive infinity. Second, we assume that the shape of the underlying parent distribution is constant through the time period with a mean value which changes linearly with time. In this way, the argument for the complementary error function can be written a function of time as follows: $x(t) = (B_0 + (\delta B/\delta t)t)/\sigma$, where $B_0 + (\delta B/\delta t)t$ is the difference from the distribution mean to the cutoff value, $(\delta B/\delta t)$ is the linear temporal change in the distribution mean, and $\sigma$ is the Gaussian width of the distribution. The magnetic measurements as plotted in Figure 3 provide support for these two assumptions.

A least-squares analysis of these three unknowns is not possible using this form because as written the argument is scale invariant. We apply one boundary condition to remove this degeneracy and to reduce the least-square fitting to just two variables, we use the mean value of the distribution from the 1998 to 2002 binning combined with the 1500 G threshold value. We then perform a least-squares fit to the sunspot formation fraction as shown in Figure 4 to determine the two parameters $(\delta B/\delta t)$ and $\sigma$. An error estimate is made by binning the sunspot formation fraction into annual bins and using the standard deviation of the values in each year; while this is only an estimate, because neither the SSN nor the F10.7 values report measurement error, it is the best that can be done. The fit returns an underlying distribution with a decreasing mean $(\delta B/\delta t) = -27 \pm 4$ Gyr$^{-1}$ and a width given by $\sigma = 500 \pm 20$ G. The resulting fit line is shown in Figure 4. The rate of change agrees with the change derived from the IR magnetic measurements by roughly $3\sigma$ but the width of the distribution is significantly broader than the width of the IR magnetic field distribution.

By extrapolating our sunspot formation fraction to the predicted peak of Cycle 24 (in mid-2013) the sunspot formation fraction would be approaching 0.5. This suggests a rather small SSN for this cycle, in agreement with some recent Cycle 24 predictions (Svalgaard et al. 2005; Hathaway 2012). And while there is no physical mechanism which suggests that we should extrapolate further, it is fascinating to see that the sunspot formation fraction would drop below 0.2 by 2020. This would suggest that although magnetic flux would be erupting at the solar surface during Cycle 25, only a small fraction of it would be strong enough to form visible sunspots or pores. Such behavior would be highly unusual, since such a small solar maximum has not been observed since the Maunder Minimum. During that period from roughly 1645 to 1715, few sunspots were observed, although cosmic-ray studies suggest the Sun did have a functioning magnetic activity cycle (Usoskin et al. 2001); this is consistent with the scenario provided by our fit extrapolation. A recent study of sunspot records suggests that the Maunder Minimum began with two small sunspot cycles with roughly the same amplitude as predicted by our extrapolation for Cycle 25 (Vaquero et al. 2011). Finally, it is interesting to note that there seems to be a strange lack of the normal precursors for Cycle 25 as observed with helioseismic and coronal emission line indicators (Hill et al. 2011; Altrock 2011).

*Facility:* McMath-Pierce

## REFERENCES

Altrock, R. C. 2011, BAAS, 43, 18.04
Bahcall, J. N., Field, G. B., & Press, W. H. 1987, ApJ, 320, L69
Bruls, J. H. M. J., Lites, B. W., & Murphy, G. A. 1991, in Solar Polarimetry, ed. L. J. November (Sunspot, NM: National Solar Observatory), 444
Fontenla, J. M., Balasubramaniam, K. S., & Harder, J. 2007, ApJ, 667, 1243
Hathaway, D. 2012, Solar Cycle 24 Prediction, http://solarscience.msfc.nasa.gov/predict.shtml
Hill, F., Howe, R., Komm, R., et al. 2011, BAAS, 43, 16.10
Johnson, R. W. 2011, Ap&SS, 332, 73
Kobel, P., Solanki, S. K., & Borrero, J. M. 2011, A&A, 531, A112
Lagg, A., Solanki, S. K., Riethmüller, T. L., et al. 2010, ApJ, 723, L164
Livingston, W. 2002, Sol. Phys., 207, 41
Maltby, P., Avrett, E. H., Carlsson, M., et al. 1986, ApJ, 306, 284
Mathew, S. K., Martínez Pillet, V., Solanki, S. K., & Krivova, N. A. 2007, A&A, 465, 291
Penn, M. J., & Livingston, W. 2006, ApJ, 649, L45
Penn, M. J., & Livingston, W. 2011, in IAU Symp. 273, The Physics of Sun and Star Spots, ed. D. Choudhary & K. Strassmeier (Cambridge: Cambridge Univ. Press), 126
Penn, M. J., & MacDonald, R. K. D. 2007, ApJ, 662, L123
Pevtsov, A. A., Nagovitsyn, Y. A., Tlatov, A. G., & Rybak, A. L. 2011, ApJ, 742, L36
Press, W. H., Teukolsky, S. A., Vetterling, W. T., & Flannery, B. P. 1992, Numerical Recipes in C (2nd ed.; Cambridge: Cambridge Univ. Press)
Rezaei, R., Beck, C., & Schmidt, W. 2012, A&A, 541, A60
Schad, T., & Penn, M. 2010, Sol. Phys., 262, 19
Stenflo, J. O., Solanki, S. K., & Harvey, J. W. 1987, A&A, 173, 167
Svalgaard, L., Cliver, E. W., & Kamide, Y. 2005, Geophys. Res. Lett., 32, L01104
Tapping, K. F., & DeTracey, B. 1990, Sol. Phys., 127, 321
Thompson, R., IPS, http://www.ips.gov.au/Educational/2/2/5
Usoskin, I. G., Mursula, K., & Kovaltsov, G. A. 2001, J. Geophys. Res., 106, 16039
Vaquero, J. M., Gallego, M. C., Usoskin, I. G., & Kovaltso, G. A. 2011, ApJ, 731, L24
Watson, F., & Fletcher, L. 2011, in IAU Symp. 273, The Physics of Sun and Star Spots, ed. D. Choudhary & K. Strassmeier (Cambridge: Cambridge Univ. Press), 51
Wesolowski, M. J., Walton, S. R., & Chapman, G. A. 2008, Sol. Phys., 248, 141